



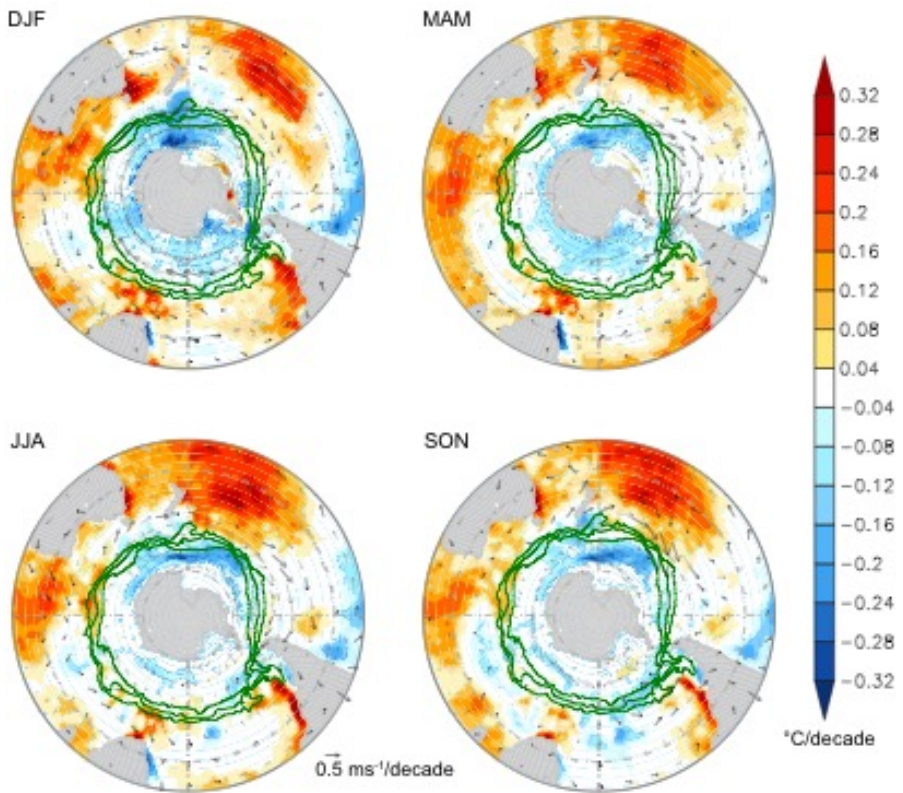
Supplement of

Tropical forcing of increased Southern Ocean climate variability revealed by a 140-year subantarctic temperature reconstruction

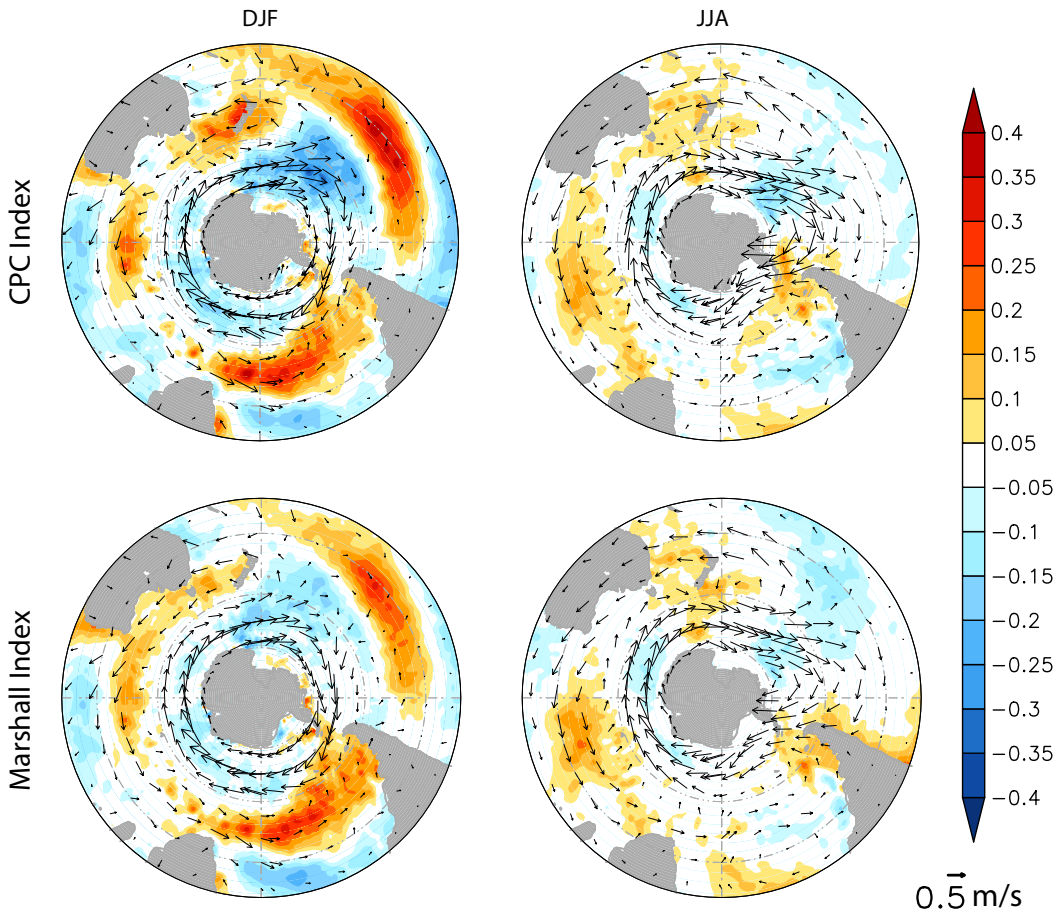
Chris S. M. Turney et al.

Correspondence to: Chris S. M. Turney (c.turney@unsw.edu.au)

The copyright of individual parts of the supplement might differ from the CC-BY 3.0 licence.



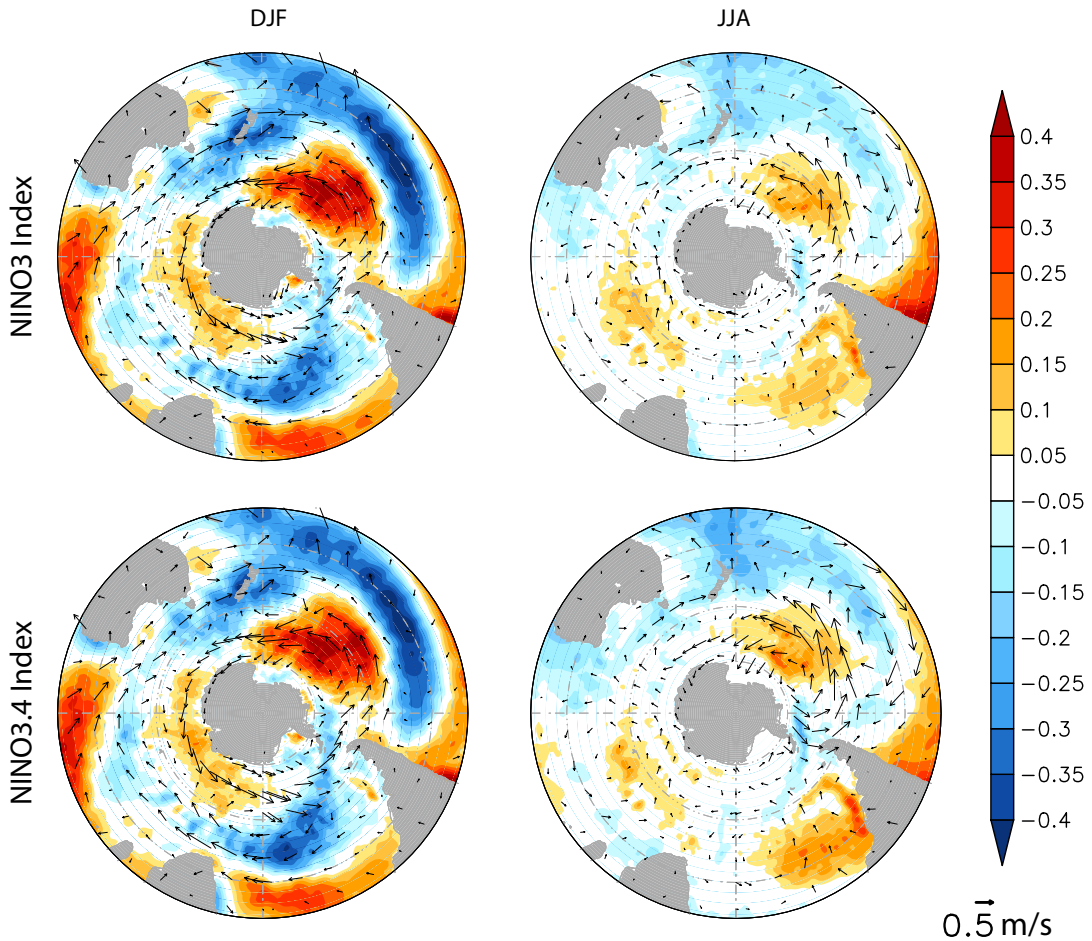
1
2 **Figure S1:** Significant ($p < 0.05$) trends in sea surface temperature (SST $^{\circ}\text{C}/\text{decade}$;
3 shading) and 925-hPa winds (vectors) for December–February (DJF), March–May
4 (MAM), June–August (JJA) and September–November (SON) since 1979.
5 Temperatures based on SSTs from the HadISST dataset (Rayner et al., 2003); winds
6 from ERA Interim (Dee et al., 2011). Overlaid in green are the main fronts of the
7 Antarctic Circumpolar Current (Sallée et al., 2012).



8

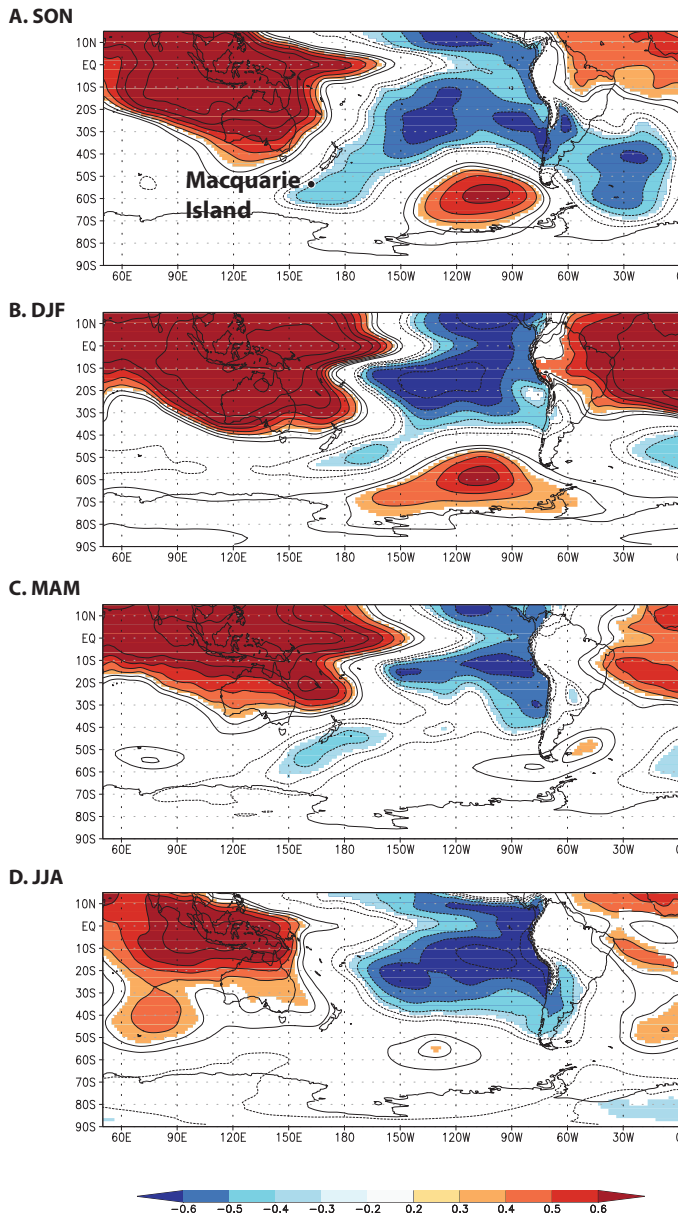
9 **Figure S2:** Austral summer (December–February) and winter (June–August) mean
10 regressions of sea surface temperature (SST) and 925-hPa winds (vectors) onto
11 different indices of the Southern Annular Mode (SAM) since 1979: the Climate
12 Prediction Centre (CPC)
13 (http://www.cpc.ncep.noaa.gov/products/precip/CWlink/daily_ao_index/ao/aao.shtml
14 l) and Marshall (2003). The results are consistent with similar analyses reported by
15 Ciasto and Thompson (2008).

16



17

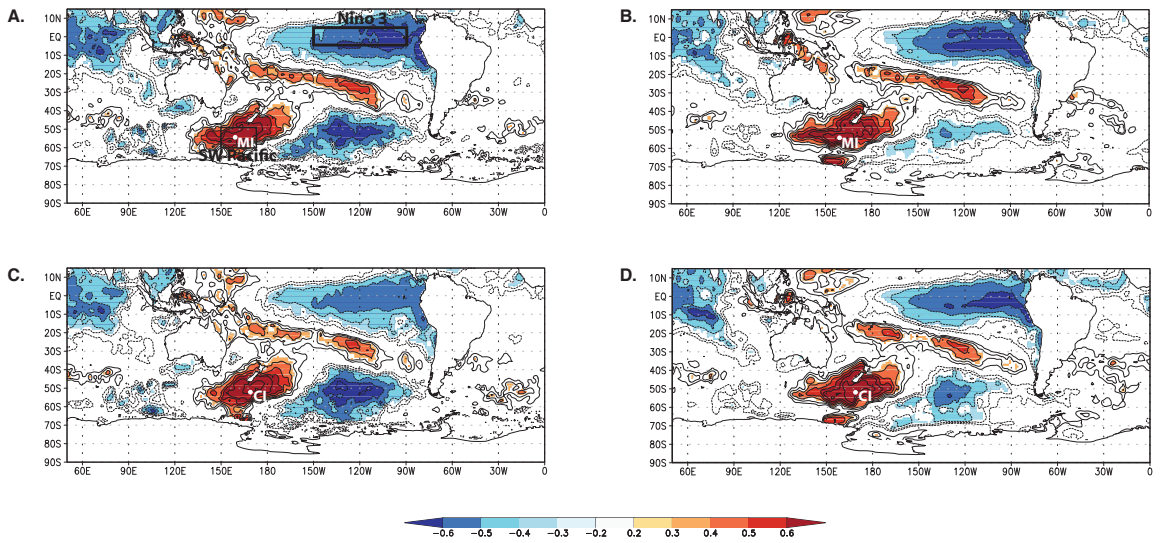
18 **Figure S3:** Austral summer (December–February) and winter (June–August) mean
 19 regressions of sea surface temperature (SST) and 925-hPa winds (vectors) onto the
 20 Niño 3 and Niño 3.4 regions of the El Niño–Southern Oscillation since 1979. The
 21 results are consistent with similar analyses reported by Ciasto and Thompson (2008).



22

23 **Figure S4:** Statistically significant spatial correlations between detrended and
 24 deseasonalised Niño 3 sea surface temperature ($p_{field} < 0.05$) (Rayner et al., 2003) and
 25 850 hPa height anomalies for September-November (SON) (A.), December-February
 26 (DJF) (B.), March-May (MAM) (C.), and June-August (JJA) (D.) using ERA Interim
 27 (Dee et al., 2011) for the period 1979-2015. Note: the tropical teleconnection is most
 28 strongly expressed at high latitudes during the austral spring and summer.

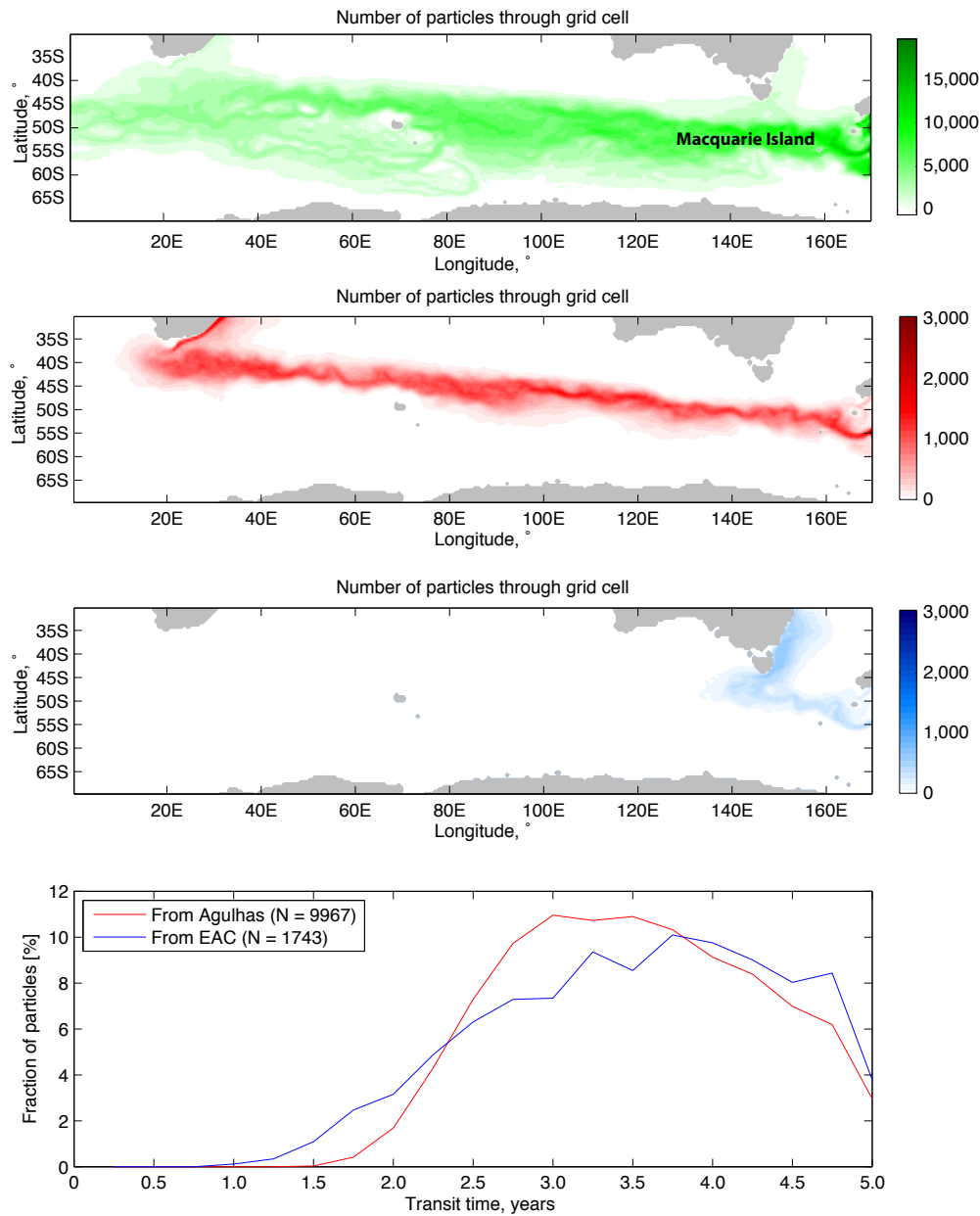
29



30

31 **Figure S5:** Spatial correlations between detrended and deseasonalised Macquarie
 32 Island and Campbell Island mean monthly atmospheric temperatures (October-
 33 March) and sea surface temperature obtained using HadISST for the period 1979-
 34 2013 (Rayner et al., 2003) (Panels A and C respectively) and Reynolds v2 for the
 35 period 1982-2013 (Smith and Reynolds, 2005) (Panels B and D) ($p_{field} < 0.05$). The
 36 southwest Pacific (SW Pacific; 50-60°S, 150-170°E) and Nino 3 regions also shown.

37



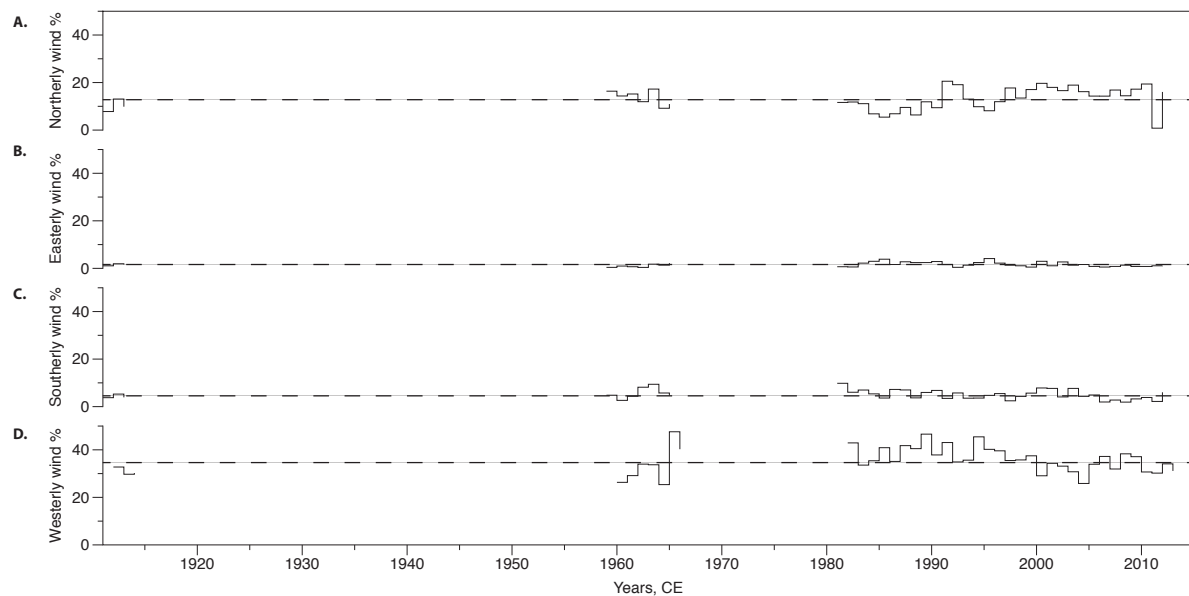
38

39 **Figure S6:** Reverse pathway of the Antarctic Circumpolar Current (A.), Agulhas (B.)
 40 and East Australian (C.) current particles that reach the southwest subantarctic region
 41 east of 170°E and south of 45°S and transit time (D.). Note that the color axis for the
 42 number of particles in Panel A. is different to Panels B. and C. Analysis undertaken
 43 using Lagrangian particles in the eddy-resolving Japanese Ocean model For the Earth
 44 Simulator (OFES) (Masumoto et al., 2004).



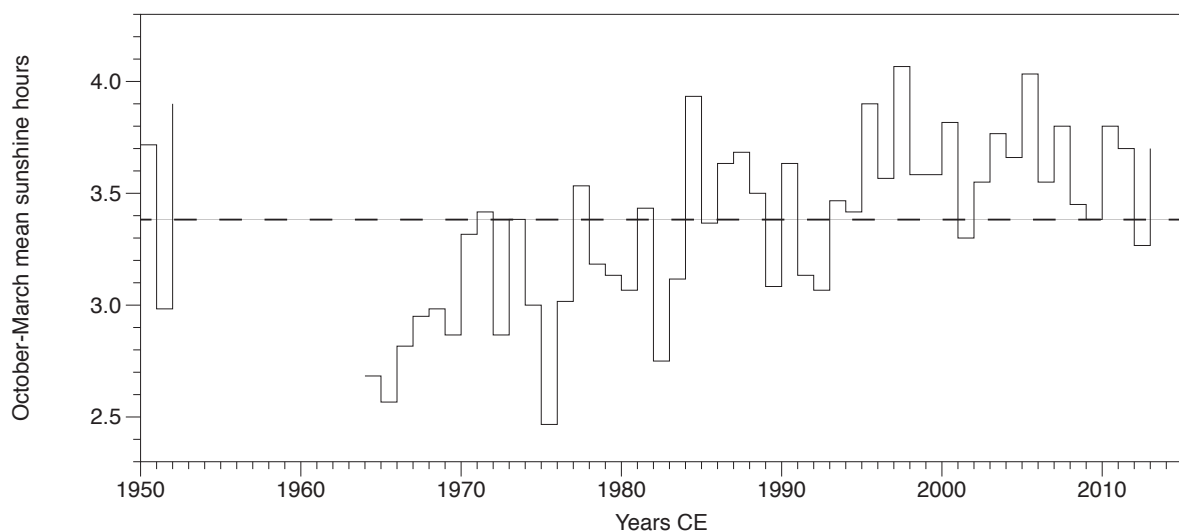
45

46 **Figure S7:** Area under the graph calculated from monthly mean temperatures obtained from
47 Macquarie Island and expressed relative to the AAE period (1912-1915).



48

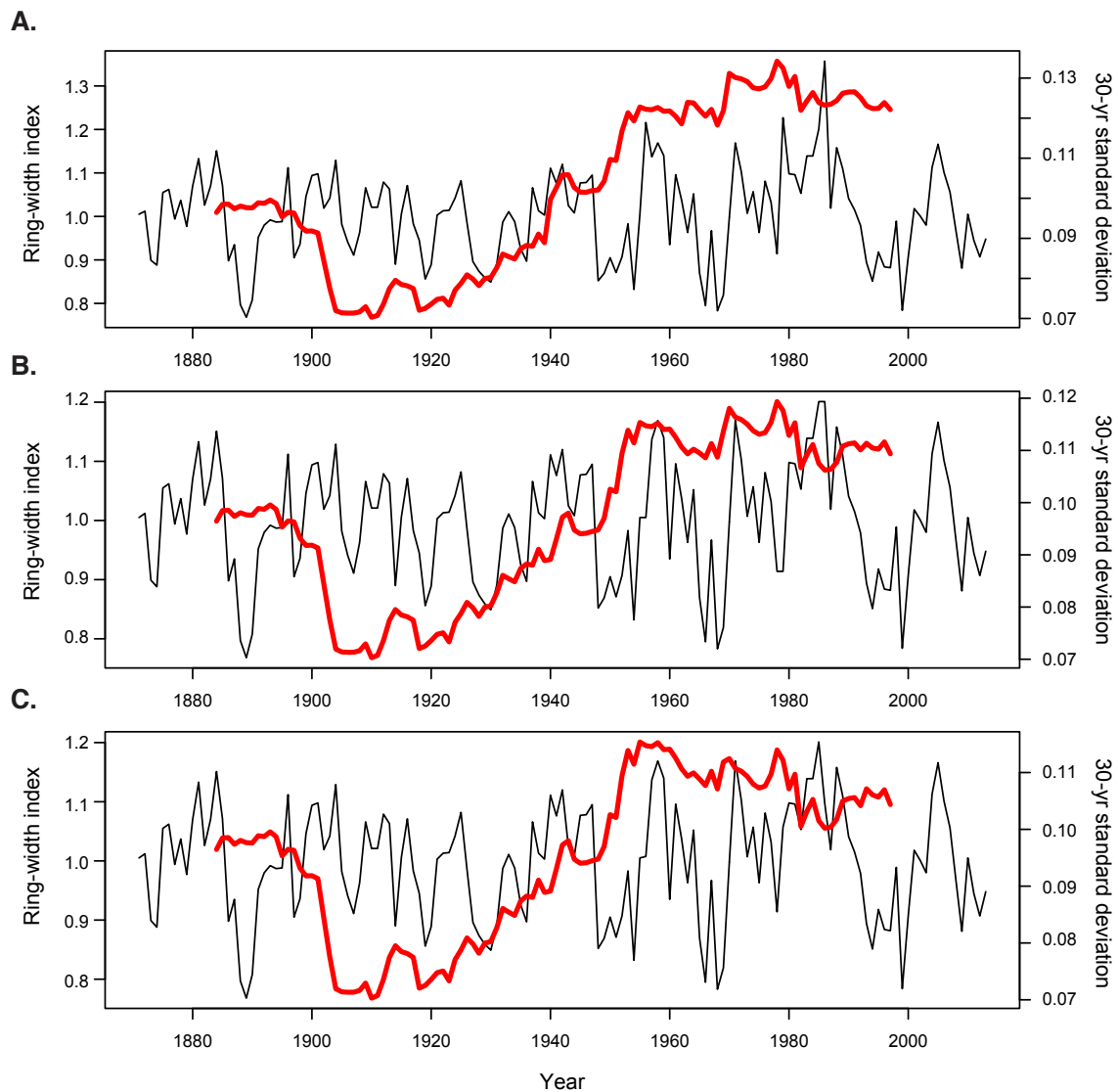
49 **Figure S8.** Percentage of austral spring-summer averaged (October-March) wind directions
50 for the four principal meridians over Macquarie Island: northerly (Panel A.), easterly (Panel
51 B.), southerly (Panel C.) and westerly (Panel D.) winds (source: Bureau of Meteorology).
52 Dashed lines denote mean values.



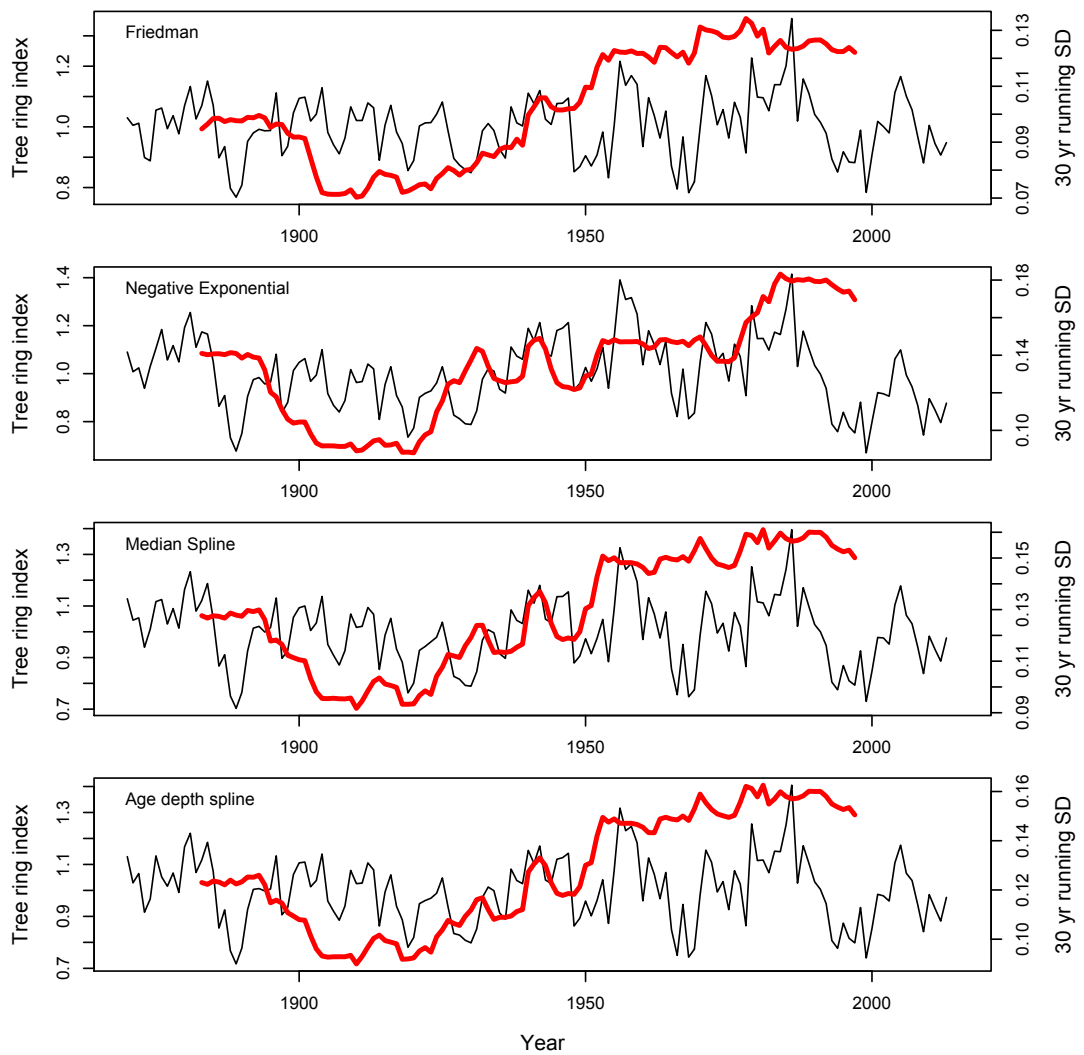
53

54 **Figure S9.** October-March mean daily sunshine hours at Macquarie Island (source: Bureau of

55 Meteorology). Dashed line denotes mean value.



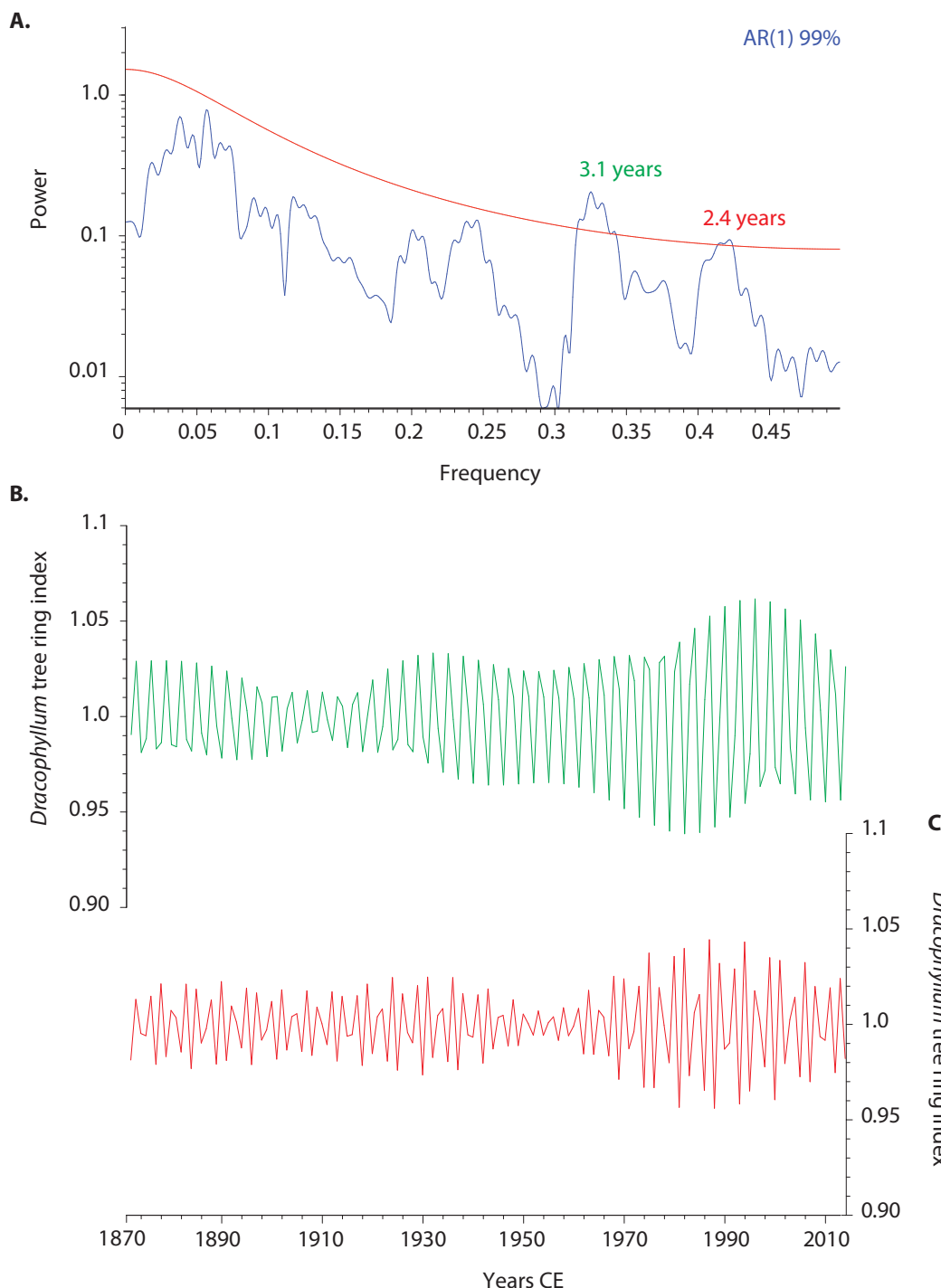
56
57 **Figure S10:** Friedman standardised *Dracophyllum* tree-ring chronology showing original data
58 (black line) and running 30-year standard deviation (red line) (A.), values extreme year values
59 from 1956, 1979 and 1986 removed and the previous year's data point duplicated (B.), and
60 extreme year values removed and replaced with the decadal average (C.). Regardless of the
61 extreme values during 1956, 1979 and 1986, the 30-year standard deviation trend remains the
62 same.
63



64

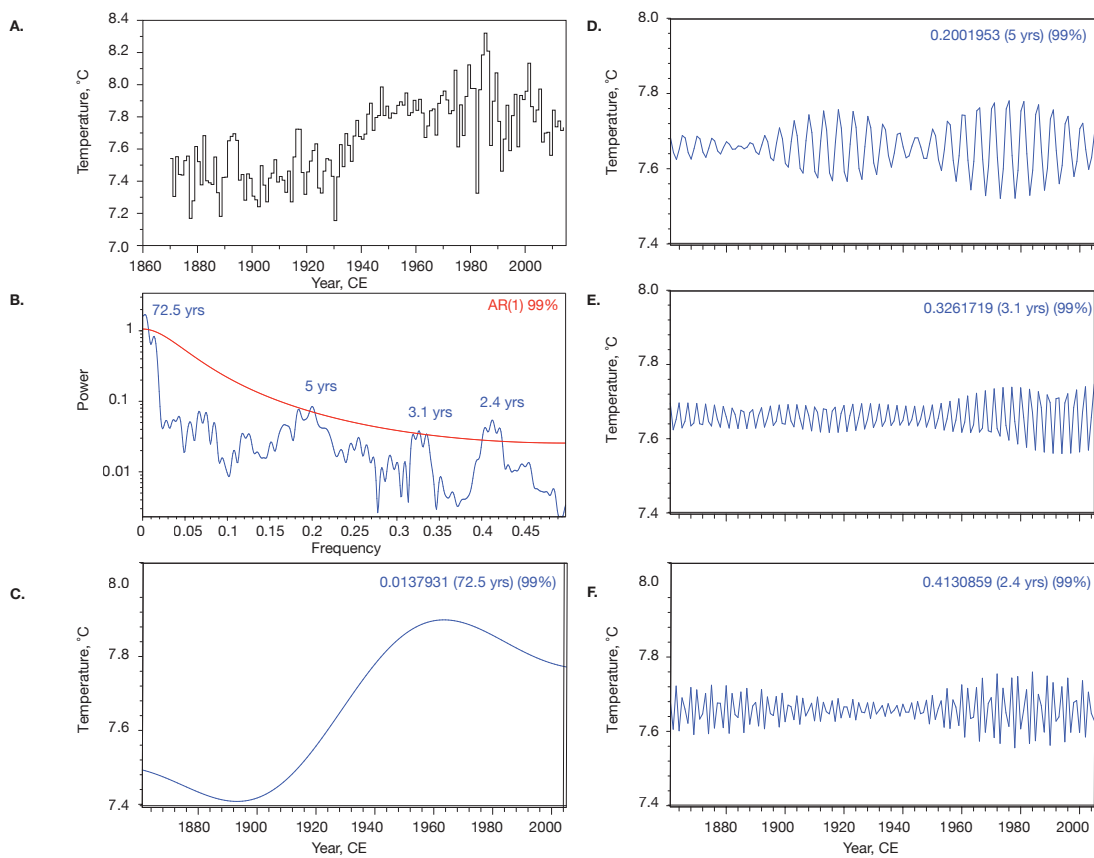
65 **Figure S11:** Comparison of the 30-year running standard deviation (red lines) for the
66 different tree-ring index standardisation methods (black lines).

67



68

69 **Figure S12:** Multi-Taper Method (MTM) (Panel A.) and extracted periodicities exceeding
 70 99% significance (Panels B. and C.) observed in the standardized *Dracophyllum* tree-ring
 71 series from Campbell Island since CE 1870.



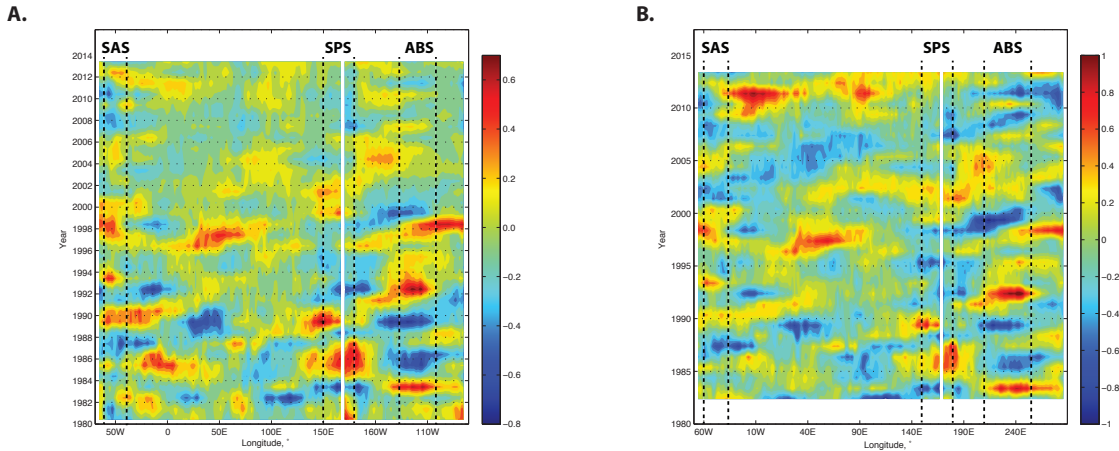
72

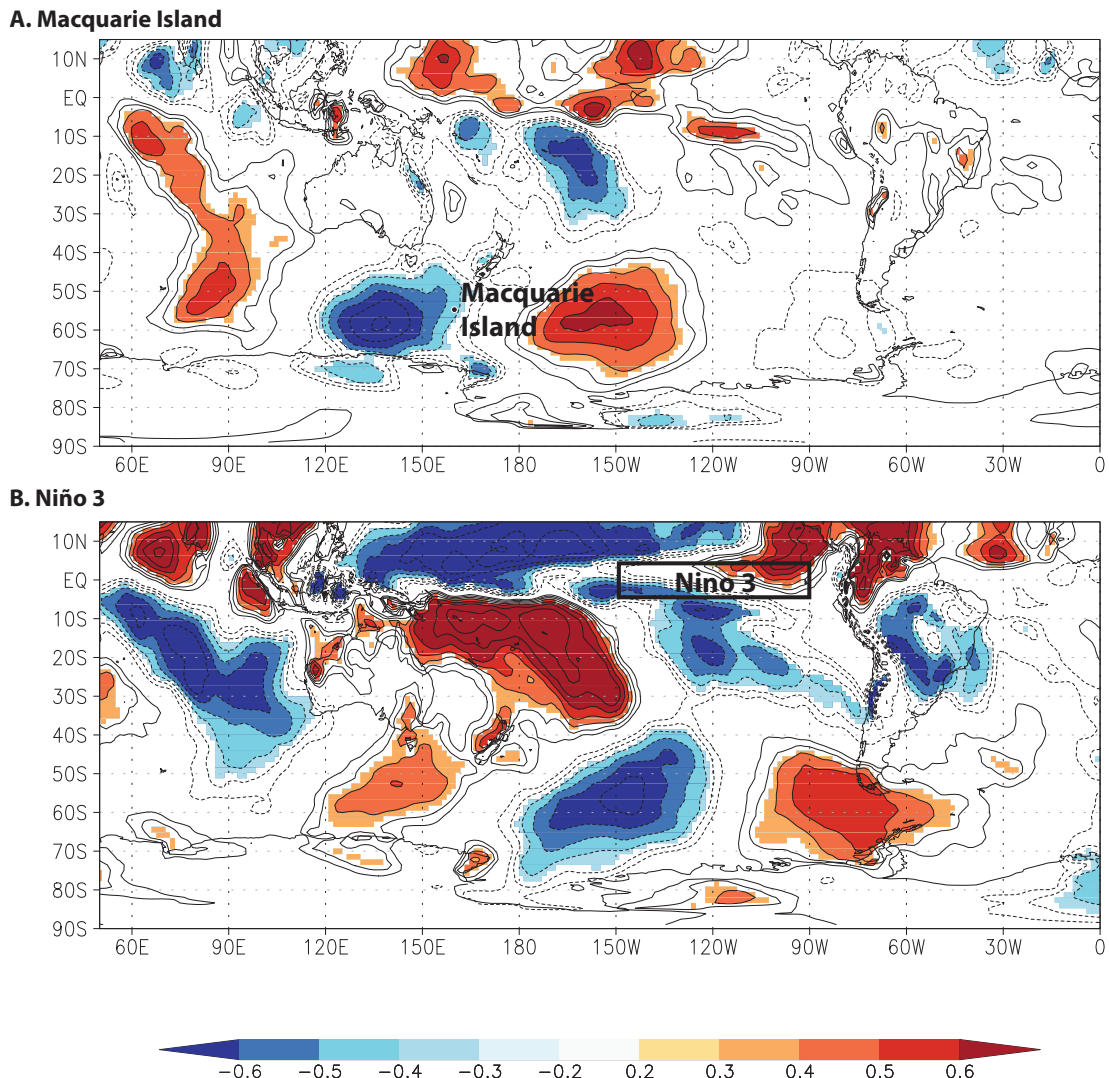
73 **Figure S13:** Annual (July-June) southwest Pacific Southern Ocean sea surface temperatures
 74 (derived from HadISST) (Rayner et al., 2003) since CE 1870 (Panel A.) with spectral analysis
 75 using Multi-Taper Method (MTM) (Panel B.) and extracted climate periodicities exceeding
 76 99% significance (Panels C.-F.).

77

78

79 **Figure S14:** Hovmöller plots showing annual temperature anomaly, meridionally averaged
80 between 45° and 55°S ($^{\circ}\text{C}$) using the HadISST (Panel A.) (Rayner et al., 2003) and the
81 Reynolds v2 (Panel B.) (Smith and Reynolds, 2005) SST datasets for the periods 1979 to
82 2014 and 1982 to 2014 respectively. The longitudes of dominant temperature changes across
83 the southwest Pacific subantarctic islands (SPS), the Amundsen and Bellingshausen seas
84 (ABS) and the south Atlantic subantarctic islands (SAS) are shown.



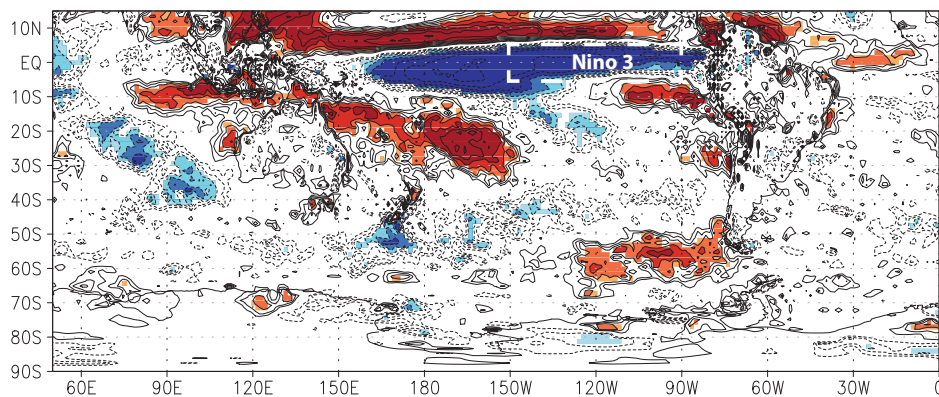


85

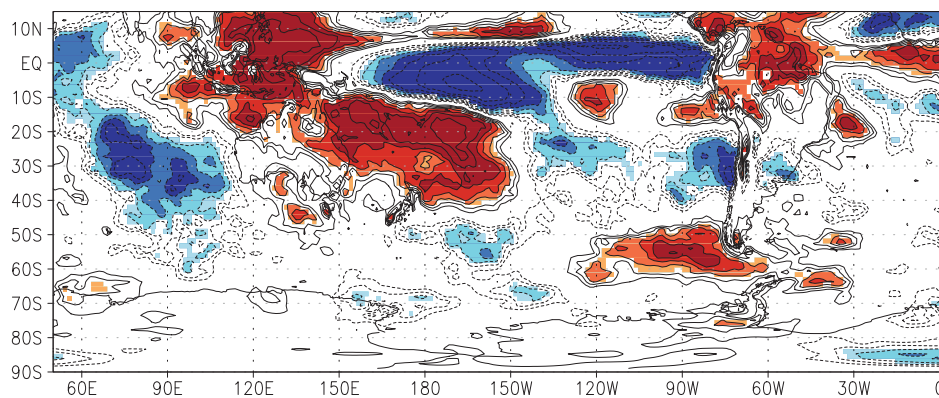
86 **Figure S15:** Spatial correlation between deseasonalized and detrended Macquarie Island (A.)
 87 and Niño 3 (B.) (October-March) temperatures and meridional wind stress (850 hPa) (ERA
 88 Interim; 1979 to 2013) (Dee et al., 2011). Significance $p_{field} < 0.05$. Note: positive correlations
 89 identify regions of enhanced southerly airflow, blue, more northerly airflow.

90

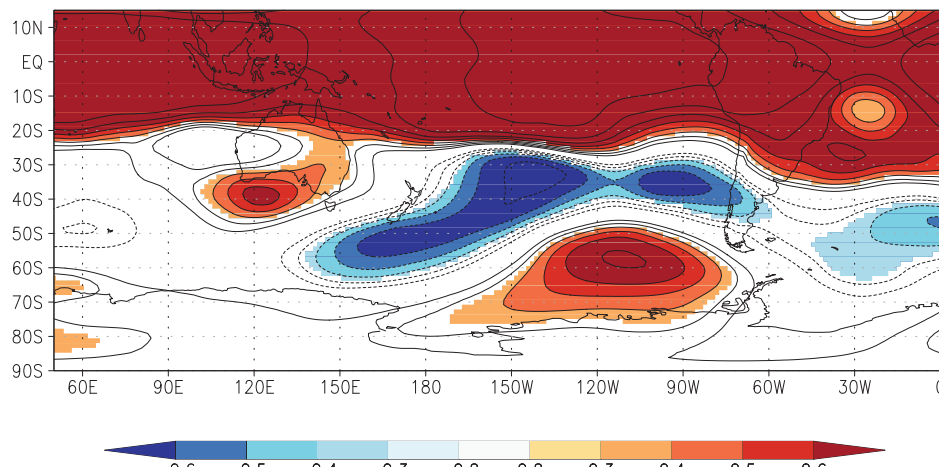
A. 850 hPa



B. 300 hPa

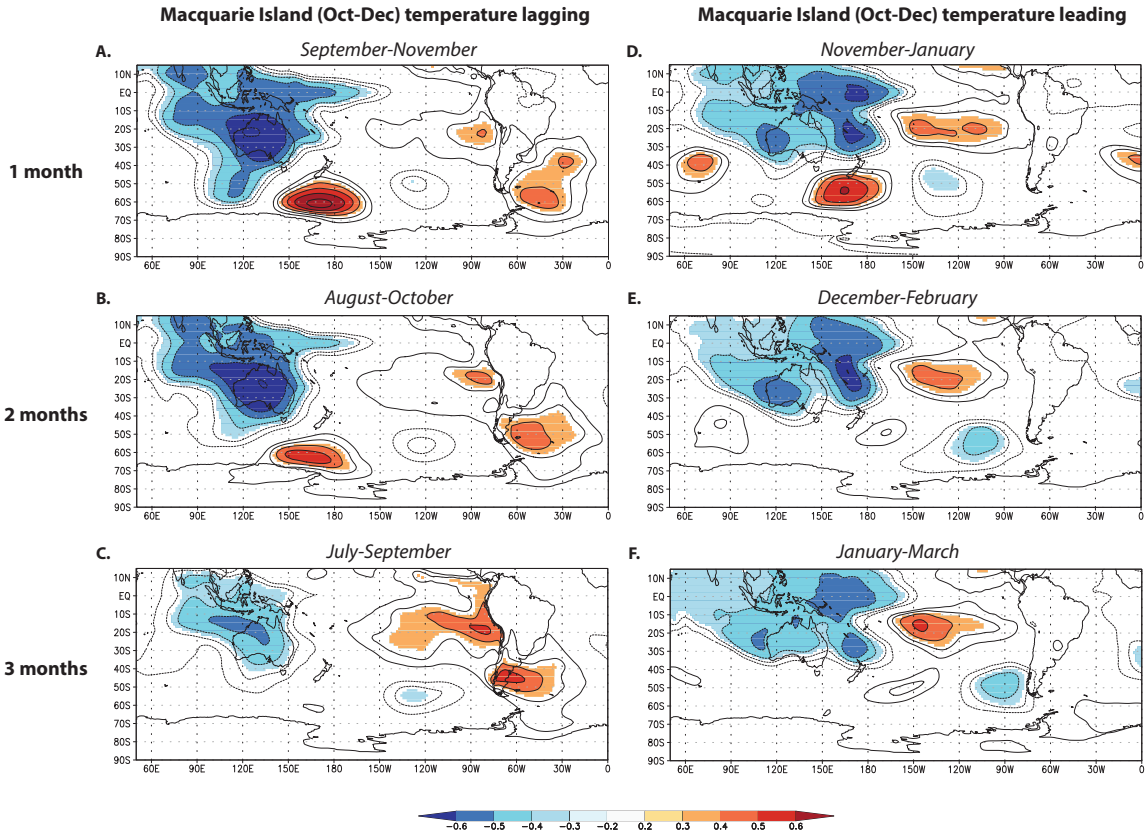


C. 300 hPa

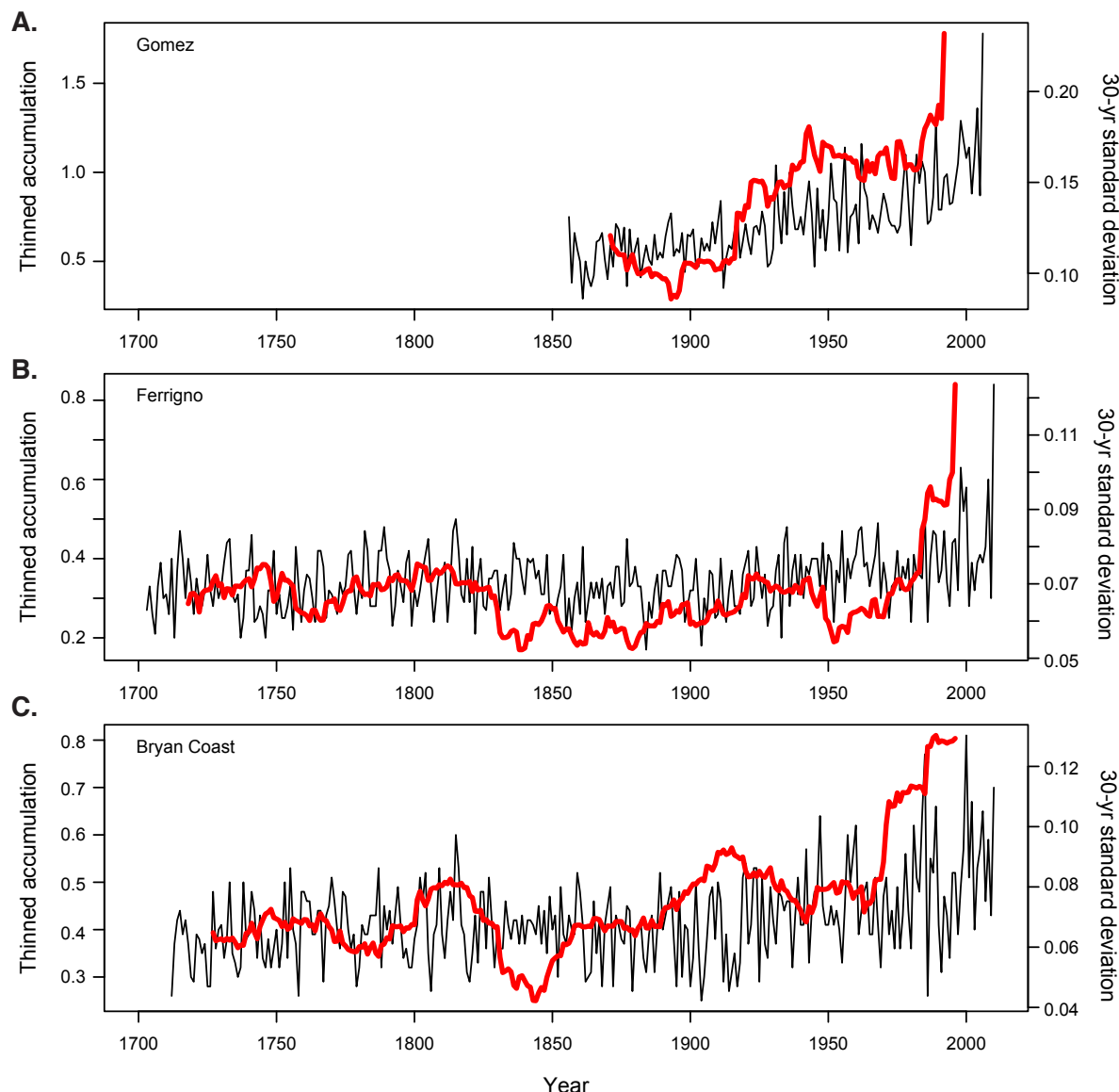


91

92 **Figure S16:** Spatial correlation between detrended and deseasonalised Nino 3 sea surface
93 temperature (Rayner et al., 2003) (October-March) and 850 hPa (A.) and 300 hPa (B.) vertical
94 velocity and 300 hPa height anomalies (C.) using ERA Interim (Dee et al., 2011) for the
95 period 1979-2015. Significance $p_{field} < 0.05$. Note: negative values indicate ascent during
96 warm SST anomalies in Nino 3.



97
98 **Figure S17:** Spatial correlation between detrended and deseasonalised Macquarie Island air
99 temperature (October-December) and 850 hPa height anomalies lagging one (A.), two (B.)
100 and three (C.) months and leading one (D.), two (E.) and three (F.) months using ERA
101 Interim(Dee et al., 2011) for the period 1979-2014. Significance $p_{field} < 0.05$.



102

103 **Figure S18:** Thinned accumulation in West Antarctic coast ice cores Gomez (A.), Ferrigno
 104 (B.) and Bryan Coast (C.) (Thomas et al., 2008; Thomas et al., 2015) with running 30-year
 105 mean standard deviation (red line).

Campbell Island: Observations (#6172)

	<i>Start</i>	<i>End</i>	<i>Count (days)</i>	<i>Percent</i>
Daily mean sea level pressure	1941-07	1995-08	19719	100
Daily surface wind	1941-07	1995-08	19760	100
Daily air temperature	1941-07	1995-08	19762	100
Campbell Island: AWS (#6174)				
	<i>Start</i>	<i>End</i>	<i>Count (days)</i>	<i>Percent</i>
Daily mean sea level pressure	1991-10	continuing	9018	100
Daily surface wind	1991-10	continuing	9018	100
Daily air temperature	1991-10	continuing	9025	100
Macquarie Island				
	<i>Start</i>	<i>End</i>	<i>Count (days)</i>	<i>Percent</i>
Daily mean sea level pressure	1948-05	continuing	24624	98.6
Daily surface wind	1948-05	continuing	24624	98.6
Daily air temperature	1948-05	continuing	24624	98.6

106

107 **Table S1:** Summary of mid to late twentieth century Campbell Island and Macquarie Island
 108 climate data including duration of record (year and month) and percentage complete (sources:
 109 Bureau of Meteorology and the New Zealand National Climate Database). Stations were
 110 inspected and serviced annually. The ‘Percent’ values provide the completeness of
 111 observations averaged over all months of record for the given station and observation type.
 112 An automatic weather station (AWS; station number #6174) was installed on Campbell Island
 113 in 1990. Sensor and site history of the Campbell Island stations #6172 and #6174 reveal no
 114 significant data interruptions. For Macquarie Island the small amount of missing data (1.4%)
 115 was mostly during the period CE 1948-1951. No complete months are missing from any of

116 the datasets. The early twentieth century AAE data from Macquarie Island (1912-1915) can
117 be obtained from Newman (1929).

	July	Aug	Sept	Oct	Nov	Dec	Jan	Feb	Mar	April	May	June	Annual
<i>AAE</i>													
1912-1915	2.8	3.1	3.2	3.1	4.3	5.8	6.3	6.1	5.6	4.6	3.8	2.8	4.3
<i>Bureau of Meteorology</i>													
1949-1952	3.3	2.6	3.3	3.4	4.3	6.0	6.5	5.9	5.5	4.7	3.8	2.9	4.4
1953-1956	2.6	3.0	2.7	4.0	4.5	6.2	7.0	6.4	6.0	5.2	4.5	2.9	4.6
1957-1960	2.9	3.3	3.5	3.9	4.6	5.6	6.8	6.8	6.1	5.3	3.7	3.1	4.6
1961-1964	2.8	2.8	3.4	4.1	4.3	5.8	6.4	6.5	5.7	4.8	3.6	3.2	4.4
1965-1968	3.1	3.6	3.5	3.2	4.2	5.5	6.7	6.6	6.4†	5.1	4.4	3.8*	4.7
1969-1972	3.5	3.7	2.5	3.3	4.7	6.2	7.2	7.2*	6.4	5.1	4.5	3.2	4.8
1973-1976	3.1	3.1	3.7	3.7	4.8	6.7	7.3	7.1*	6.6	5.3*	3.7	3.1	4.8*
1977-1980	4.3*	4.0*	3.9	4.1	4.5	6.2	7.4	7.5	6.8*	5.7*	4.7	3.7	5.2†
1981-1984	3.5	3.3	3.7	4.0	4.6	6.0	6.8	7.0	6.7	5.4	4.6	3.8*	4.9

1985-1988	3.4	3.5	3.3	4.5	5.2	6.7	7.9*	8.0*	6.7	5.5*	3.8	3.1	5.1*
1989-1992	3.6	3.3	4.0	4.2	5.0	5.8	7.5	6.9	6.2*	5.2	4.0	3.6	4.9
1993-1996	2.6	3.2	3.3	3.7	4.6	5.9	6.9	7.1*	6.6*	5.8*	4.6	2.7	4.7
1997-2000	3.6	3.1	4.2	4.0	4.5	6.1	7.0	7.1	6.1	5.0	4.5	3.6	4.9*
2001-2004	3.6	3.4	3.5	4.1	5.0	6.0	7.4	7.1	6.5†	5.7†	3.9	3.3	4.9*
2005-2008	2.9	3.6	3.5	3.8	4.4	6.6	7.1	7.2*	6.5†	5.8*	4.7	3.3	4.9*
2009-2012	2.8	3.7	3.8	3.6	3.8	6.1	7.0	7.0*	6.4*	5.8*	4.9	3.2	4.8*

119

120 **Table S2:** Four-year binned monthly atmospheric temperatures for the Isthmus, Macquarie Island. Statistically-significant two-tailed t-tests121 differences between the modern record and the original Australasian Antarctic Expedition (AAE) are given in bold: * $p<0.05$ and † $p<0.01$.

122

	July	August	September	October	November	December	January	February	March	April	May	June	Annual
<i>AAE</i>													
1912-													
1915	3.4	3.6	3.8	4.1	5.1	6.3	6.6	5.7	5.3	4.8	3.9	3.5	4.7
<i>Loewe</i>													
1951-													
1954	3.6	3.5	3.8	3.8	5.4	6.7	7.3	7.2	6.7	5.8	4.7	3.8	5.2
1957,													
1962-													
1964	4.2	4.2	4.4	4.6	5.4	5.4	7.0	6.7	6.1	5.5	4.7	4.2	5.2
<i>MODIS</i>													
2001-													
2004	2.9	3.5	3.6	3.9	4.3	5.9	7.1	6.9	6.8*	5.3	5.4*	2.7	4.8
2005-													
2008	2.7	2.7	4.4	3.9	4.6	5.8	6.4	7.0*	6.4*	5.8	5.0	3.8	4.9

2009-

2012 3.4 4.3 4.1 4.6 4.8 5.8 6.7 **7.5*** **6.9*** 5.3 4.3 3.0 5.0

123

124 **Table S3:** Four-year binned monthly sea surface temperature (SST) for Buckles Bay, Macquarie Island. Statistically-significant two-tailed t-
125 differences between the SSTs obtained during the 1950s and 1960s (Loewe, 1968, 1957) and MODIS 4 km-resolved 11 μm daytime satellite
126 observations to the original Australasian Antarctic Expedition (AAE) are given in bold: * $p<0.05$. Note, the 1950s and 1960s SSTs obtained from
127 Macquarie Island are reported as monthly averages by Loewe (1957, 1968), precluding t-tests.

Dracophyllum - Campbell Island temperature (°C, October-March)

Calibration Period	Variance Explained (%)	Pearson Correlation (r)	RE	Verification Period	Pearson Correlation (r)	RE	CE
"Early" 1949-1980	29.9	0.547	0.299	1981-2012	0.552	0.342	0.245
1st-differenced		0.571	0.285		0.619	0.298	0.297
"Late" 1981-2012	28.4	0.533	0.284	1949-1980	0.562	0.410	0.234
1st-differenced		0.639	0.323		0.542	0.289	0.291
Entire Period (1949-2012)	31.3	0.559	0.291				

Dracophyllum - Macquarie Island temperature (°C, October-March)

Calibration Period	Variance Explained (%)	Pearson Correlation (r)	RE	Verification Period	Pearson Correlation (r)	RE	CE
"Early" 1949-1980	25.7	0.507	0.257	1981-2012	0.449	0.277	-0.003
1st-differenced		0.534	0.262		0.557	0.234	0.232
"Late" 1981-2012	22.2	0.471	0.222	1949-1980	0.524	0.370	-0.478
1st-differenced		0.571	0.258		0.532	0.283	0.283
Entire Period (1949-2012)	26.4	0.513	0.240				

128

129 **Table S4:** Calibration and verification statistics for the *Dracophyllum* tree-ring reconstruction of ‘growing-season’ temperature on Campbell

130 and Macquarie islands (October-March).

CMIP5 model	Correlation to reconstructed Macquarie Island temperature (Oct-Mar)	Significance (<i>p</i>)
ACCESS1-0	0.001	0.9946
ACCESS1-3	0.070	0.2561
bcc-csm1-1	0.026	0.6751
bcc-csm1-1-m	-0.027	0.6601
BNU-ESM	-0.054	0.6142
CanESM2	-0.071	0.1412
CCSM4	0.050	0.2574
CESM1-BGC	-0.011	0.9179
CESM1-CAM5	-0.047	0.4531
CESM1-CAM5-1-	-0.088	0.1000
FV2		
CESM1-FASTCHEM	-0.038	0.5418
CESM1-WACCM	-0.014	0.8975
CMCC-CM	-0.072	0.5002
CMCC-CMS	-0.033	0.7611
CMCC-CESM	-0.134	0.2184

CNRM-CM5	-0.037	0.2770
CSIRO-Mk3-6-0	0.003	0.9271
EC-EARTH	0.002	0.9623
FGOALS-g2	-0.048	0.3097
FIO-ESM	-0.055	0.3747
GFDL-CM3	-0.006	0.8963
GFDL-ESM2G	0.103	0.0958
GFDL-ESM2M	-0.006	0.9584
GISS-E2-H p1	0.022	0.6807
GISS-E2-H p2	0.043	0.3760
GISS-E2-H p3	-0.023	0.6019
GISS-E2-H-CC p1	0.015	0.8915
GISS-E2-R p1	-0.009	0.8338
GISS-E2-R p2	-0.038	0.3843
GISS-E2-R p3	0.008	0.8622
GISS-E2-R-CC p1	0.015	0.8915
HadGEM2-AO	-0.006	0.9555
HadGEM2-CC	-0.067	0.5319
HadGEM2-ES	-0.114	0.0300
inmcm4	0.065	0.5538

IPSL-CM5A-LR	0.001	0.9793
IPSL-CM5A-MR	-0.032	0.6135
IPSL-CM5B-LR	0.174	0.0891
MIROC5	0.120	0.0097
MIROC-ESM	0.012	0.8470
MIROC-ESM-CHEM	-0.133	0.2194
MPI-ESM-LR	0.074	0.2269
MPI-ESM-MR	0.009	0.8858
MPI-ESM-P	0.011	0.8866
MRI-CGCM3	-0.090	0.1471
MRI-ESM1	0.069	0.5295
NorESM1-M	0.052	0.6339
NorESM1-ME	0.042	0.4934

131 **Table S5:** Correlations and significance between CMIP5 modelled surface air
 132 temperatures centred over 52-57°S and 157-162°E (Taylor et al., 2011) and
 133 reconstructed Macquarie Island temperatures (detrended and deseasonalised October-
 134 March, CE 1871-2004). $p < 0.05$ given in bold. Note, HadGEM2-ES is inversely
 135 correlated and MIROC5 has a correlation of only 0.12.

136
 137

Tree-ring standardisation	F-test ratio of variances	p value	Bartlett's K-squared	p value
Friedman				
temperature	0.513	<0.0055	7.7069	<0.0055
reconstruction				
Friedman tree-ring index	0.518	<0.0061	7.5294	<0.0061
Medium spline tree- ring index				
	0.561	<0.0158	5.8285	<0.0158
Negative exponential tree-ring index				
	0.645	<0.0663	3.3752	<0.0662
Age depth spline tree-ring index				
	0.601	<0.0333	4.5363	<0.0332

138

139 **Table S6:** Comparison of the variance across the tree-ring record (CE 1870-1940 vs
 140 1941-2012), for different standardization methods and the Friedman temperature
 141 reconstruction reported here. The second half of the twentieth century is significantly
 142 larger (in all cases F and Bartlett's K-squared tests $p < 0.07$), suggesting a shift in
 143 climate to one characterised by pervasive high variability, regardless of the
 144 standardisation method used.

145

146

147

	Eastern rockhopper (<i>Eudyptes filholi</i>)	Erect crested penguin (<i>Eudyptes sclateri</i>)
1978	50,000	115,000
1995	3,392	52,000
2011	2,475	42,689

148

149 **Table S7:** Eastern rockhopper and Erect crested penguin populations on the
150 Antipodes Islands. In 1978 breeding pairs were counted whereas in 1995 and 2011
151 nests were the unit counted (Hiscock and Chilvers, 2014).

152 **References**
153
154 Ciasto, L. M., and Thompson, D. W. J.: Observations of large-scale ocean–atmosphere interaction in
155 the Southern Hemisphere, Journal of Climate, 21, 1244-1259, 10.1175/2007jcli1809.1, 2008.
156 Dee, D. P., Uppala, S. M., Simmons, A. J., Berrisford, P., Poli, P., Kobayashi, S., Andrae, U.,
157 Balmaseda, M. A., Balsamo, G., Bauer, P., Bechtold, P., Beljaars, A. C. M., van de Berg, L., Bidlot, J.,
158 Bormann, N., Delsol, C., Dragani, R., Fuentes, M., Geer, A. J., Haimberger, L., Healy, S. B., Hersbach, H.,
159 Hólm, E. V., Isaksen, L., Kållberg, P., Köhler, M., Matricardi, M., McNally, A. P., Monge-Sanz, B. M.,
160 Morcrette, J. J., Park, B. K., Peubey, C., de Rosnay, P., Tavolato, C., Thépaut, J. N., and Vitart, F.: The ERA-
161 Interim reanalysis: configuration and performance of the data assimilation system, Quarterly Journal of the
162 Royal Meteorological Society, 137, 553-597, 10.1002/qj.828, 2011.
163 Hiscock, J. A., and Chilvers, B. L.: Declining eastern rockhopper (*Eudyptes filholi*) and erect-crested
164 (*E. sclateri*) penguins on the Antipodes Islands, New Zealand, New Zealand Journal of Ecology, 38, 124-131,
165 2014.

166 Loewe, F.: A note on the sea water temperatures at Macquarie Island, Australian Meteorological
167 Magazine, 19, 60-61, 1957.
168 Loewe, F.: A further note on the sea water temperatures at Macquarie Island, Australian Meteorological
169 Magazine, 16, 118-119, 1968.
170 Marshall, G.: Trends in the Southern Annular Mode from observations and reanalyses, Journal of
171 Climate, 16, 4134-4143, 2003.
172 Masumoto, Y., Sasaki, H., Kagimoto, T., Komori, N., Ishida, A., Sasai, Y., Miyama, T., Motoi, T.,
173 Mitsudera, H., Takahashi, K., Sakuma, H., and Yamagata, T.: A fifty-year eddy-resolving simulation of the
174 world ocean – Preliminary outcomes of OFES (OGCM for the Earth simulator), Journal of the Earth Simulator,
175 1, 35-56, 2004.
176 Newman, B. W.: Meteorology. Tabulated and Reduced Records of the Macquarie Island Station,
177 Sydney, 539, 1929.
178 Rayner, N. A., Parker, D. E., Horton, E. B., Folland, C. K., Alexander, L. V., Rowell, D. P., Kent, E. C.,
179 and Kaplan, A.: Global analyses of sea surface temperature, sea ice, and night marine air temperature since the
180 late nineteenth century, Journal of Geophysical Research: Atmospheres, 108, 4407,
181 doi:10.1029/2002JD002670, 10.1029/2002JD002670, 2003.

182 Sallée, J.-B., Matear, R. J., Rintoul, S. R., and Lenton, A.: Localized subduction of anthropogenic
183 carbon dioxide in the Southern Hemisphere oceans, *Nature Geoscience*, 5, 579-584,
184 <http://www.nature.com/ngeo/journal/v5/n8/abs/ngeo1523.html> - supplementary-information,
185 2012.

186 Smith, T. M., and Reynolds, R. W.: A global merged land-air-sea surface temperature reconstruction
187 based on historical observations (1880-1997), *Journal of Climate*, 18, 2021-2036, 2005.

188 Taylor, K. E., Stouffer, R. J., and Meehl, G. A.: An overview of CMIP5 and the experiment design,
189 *Bulletin of the American Meteorological Society*, 93, 485-498, 10.1175/BAMS-D-11-00094.1, 2011.

190 Thomas, E. R., Marshall, G. J., and McConnell, J. R.: A doubling in snow accumulation in the western
191 Antarctic Peninsula since 1850, *Geophysical Research Letters*, 35, doi: 10.1029/2007GL032529,
192 10.1029/2007GL032529, 2008.

193 Thomas, E. R., Hosking, J. S., Tuckwell, R. R., Warren, R., and Ludlow, E.: Twentieth century increase
194 in snowfall in coastal West Antarctica, *Geophysical Research Letters*, 42, 9387-9393, 2015.

195